ATMOSPHERIC ATTENUATION ON HELIOSTAT FIELD

Alois Salmon[1], Mercedes Ibarra[1]

[1] Fraunhofer Chile Research, Center for Solar Energy Technologies, Santiago (Chile)

Abstract

Concentrating Solar Power design is highly dependent on local solar radiation, atmospheric variables (i.e. water vapor content, aerosols concentration, etc) and wind velocity. In the special case of central receiver power plants, the impact of atmospheric attenuation has to be taken into account to get more accurate designs. Atmospheric attenuation impacts both solar resource and heliostat field energy transmission and is neither measured nor estimated by main solar atlas. A common heliostat field design consists of overestimating heliostat number to ensure that the nominal energy is received at the receiver for all the range of attenuation values. Atmospheric attenuation is a physical process that does not impact all wavelengths in the same way and therefore it cannot be described as a single atmospheric attenuation without losing its physical meaning. This work is focused on deriving atmospheric attenuation values from ground data using a numerical model and describes step by step how it should be applied to estimate whole heliostat field attenuation. Atmospheric attenuation will first be described from the radiative transfer theory to be express for each heliostat. On a second part, numerical application will be shown using SMARTS radiative transfer model with satellite date from MERRA-II. Variation in LCOE induced by atmospheric attenuation will be calculated to show importance of this parameter in site selection for tower power plant.

Keywords: CSP, Heliostat field simulation, atmospheric attenuation, solar spectrum,

1. Introduction

On the path to the ground, sun's photons interact with atmospherics compounds (scattering and absorption) leading to a decrease of solar resource at ground level. In the case of Central Solar Receiver (CSR) technologies (like tower power plants), this atmospheric interaction may still impact the amount of reflected flux from the heliostat before reaching the tower receiver, due to the high travels distance. This attenuation mostly depends on water vapor and aerosols concentration in the atmosphere at ground level and can represent up to 30 % of losses for far heliostat (Ballestrín and Marzo, 2012). Knowing well these attenuation losses at the time of the selection of the plant location could help to reduce costs (better heliostat field design) and risks (effective solar resource well estimated).

In this work, we will study the impact of the atmospheric attenuation over a whole heliostat field taking into account different factors. First, it will be demonstrated that atmospheric attenuation between any heliostat and the tower can be written as a function of attenuation between tower and ground in a vertical path. To estimate this attenuation, SMARTS model (Gueymard, 2001) will be used to extract atmospheric transmission and furthermore calculate the total heliostat field attenuation. Finally, a method to calculate monthly or yearly heliostat field attenuation from a single point (time and space) will be detailed. Numerical calculation will be done to illustrate the theoretical method. To do so, two sites will be study in the North of Chile, one in the Atacama Desert and the other one near to the pacific cost.

2. Extinction optical depth on heterogeneous atmosphere

Photons may interact with the atmospherics' particles in two occasions when using CSR technologies. The first time is to reach the heliostat level and the second time is on the way to the tower. Those interactions lead to a decrease of the power that can be absorbed by the solar receiver. The Beer Lambert's law can summarize the link between atmospheric attenuation and transmitted power:

$$\mathcal{T}_\lambda = e^{\int_{s_1}^{s_2} -k_\lambda(s)ds} \qquad \text{(Eq. 1)}$$

doi:10.18086/swc.2019.45.09 Available at http://proceedings.ises.org

In Eq. 1, the atmospheric interactions are summarized in the extinction coefficient $k_\lambda(s)$ for a wavelength λ and position s along the path beteen two points s_1 and s_2. Knowing the value of the extinction coefficient at each point of the atmosphere would be enough to solve both the radiation reaching heliostat and the losses between its paths to the tower. Unfortunately this coefficient is usually unknown, and therefore it is hard to estimate those losses. If we suppose that the extinction coefficient is constant along the horizontal plane xOy (only depends on the height z), and that it is continue, the extinction coefficient can be solved in the plane xOz as shown in Figure 1.

$$dl = dz\sqrt{1 + \left(\frac{x_h}{z_t}\right)^2} = \alpha dz \qquad \text{(Eq. 2)}$$

If we combine Eq. 1 and Eq. 2 we can write the atmospheric attenuation between the heliostat and the tower ($\mathcal{T}_{\lambda,p_h}$) as a function of the attenuation between ground and tower in a vertical path ($\mathcal{T}_{\lambda,p_T}$):

$$\mathcal{T}_{\lambda,p_h} = e^{\int_0^{z_t} -\alpha k_\lambda(z)dz} = \left(e^{\int_0^{z_t} -k_\lambda(z)dz}\right)^\alpha = \left(\mathcal{T}_{\lambda,p_T}\right)^\alpha \qquad \text{(Eq. 3)}$$

Eq. 3 shows that if we can estimate the transmission between tower and ground level in a vertical path (numerically or experimentally measured), the whole heliostat field can be described with the same equation, changing only the value of α according to the heliostat – tower distance. To make experimental measurements of this attenuation, two spectrophotometers could be used, one at the top of the tower and one at the base, both measuring DNI spectrum. The main challenge with this experimental method could be the measurement sensitivity, as the difference between the two measurements will be very low and may be within experimental error. Hence, in the following, a method based on SMARTS will be used in order to estimate this attenuation between tower and ground level in the vertical path. Note that the factor α from Eq. 2 represents the increment of length between heliostat and tower in proportion of high of tower.

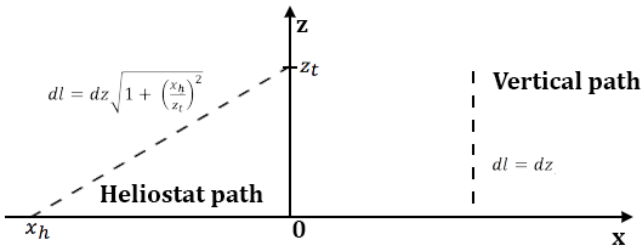

Figure 1 Integration path from heliostat to tower and from ground to tower in a vertical way.

3. Heliostat field extinction

Using Eq. 3, the local attenuation for any heliostat can be written as the integration of the attenuation spectrum in a vertical path between ground and tower. If we want to use a plant scale attenuation (ie. only one value to describe the whole power plant), each local attenuation has to be summed, taking into account all individual cosine effect, blocking and shading.

Using Eq. 3 for each heliostat allows the calculation of the whole heliostat field attenuation for each wavelength λ but the attenuation losses, in percent of DNI power, is often used to design power plants (NREL, 2014). This attenuation losses need to be calculated using the current DNI spectrum and Eq. 3. Main drawbacks of this calculation reside in the integral form of the transmittance. Indeed, as shown by Eq. 4, due to exponential dependency on wavelength, the transmittance of a heliostat cannot be written, in general, as a product of the spectral transmittance of any other heliostat (or ground-tower) transmittance by the DNI.

$$\mathcal{T}_\alpha = \int_{\lambda_{min}}^{\lambda_{max}} DNI_\lambda e^{-\alpha\tau_\lambda} d\lambda \;\Leftrightarrow\; DNI \left(\int_{\lambda_{min}}^{\lambda_{max}} e^{-\tau_\lambda} d\lambda\right)^\alpha \quad \text{(Eq. 4)}$$

Therefore, atmospheric losses at a slant-distance $\alpha * z_t$ of the tower has to be written:

$$\mathcal{A}_\alpha = 1 - \frac{\int_{\lambda_{min}}^{\lambda_{max}} \rho_{\lambda^*}\ DNI_{\lambda^*} e^{-\alpha\tau_\lambda} d\lambda}{\int_{\lambda_{min}}^{\lambda_{max}} \rho_{\lambda^*} DNI_\lambda d\lambda} \quad \text{(Eq. 5)}$$

Where ρ_λ is the spectral reflectivity of the heliostat and DNI_λ the value of DNI at the wavelength λ. Note that the reflectivity is used in both numerator and denominator to take into account only atmospheric losses in the equation and not reflectivity losses. The full losses for an heliostat, h, can be written:

$$\mathcal{A}_{\alpha,h} = 1 - \frac{\int_{\lambda_{min}}^{\lambda_{max}} \rho_{\lambda^*}\ DNI_{\lambda^*} e^{-\alpha\tau_\lambda} d\lambda}{\int_{\lambda_{min}}^{\lambda_{max}}\ DNI_\lambda d\lambda} * \beta \quad \text{(Eq. 6)}$$

Where β is a dimensionless coefficient taking into account cosine effect, blocking and shading losses, supposed to be independents of the wavelength.

4. Numerical application

The implementation of the theoretical method has been employed by using SMARTS with satellite data to describe the atmosphere at two sites in Chile. The two sites almost share same latitude but the first site (Point 1) is close to the Pacific sea while the second (Point 2) is located into the Atacama Desert of Chile. The elevation is also different has first site (Point 1) is 80 meters above sea level while second site (Point 2) is at more than 2700 meters above sea level. Table 1 shows main characteristics of the two sites used in this study.

Tab. 1: Locations of the two sites used to illustrate the numerical calculation of atmospheric attenuation.

Site name	Site characteristics	Latitude [°]	Longitude. [°]	Elevation [m]
Point 1	Maritime	-23.00	-71.25	80
Point 2	Desert	-23.5	-68.875	2780

The MERRA-II (Bosilovich et al., 2015) database related to aerosols properties (Aerosol Optical Depth at 550 nm), total content of water (TCW), total ozone content (TOC) and ground pressure has been used as input of SMARTS model to estimate atmospheric attenuation. As this work only aims to demonstrate the feasibility of the theoretical method proposed, the atmospheric vertical profile has been set to the US-Standard and the aerosol model Rural has been chosen and the simulated tower is 200 meter above ground level. The Sandia method (Ebrahimpour and Maerefat, 2010) has been applied to the MERRA-II database, for 30 years of data from 1989 to 2018, to get the most representative year of aerosols optical depth by selection of representative months.

Once all the atmospheric description was obtained, two different simulations were done with SMARTS model to obtain spectral transmittance between tower and ground along a vertical path and to obtain DNI spectrum at ground level for the current sun's position. As already used by Gueymard et al. (2017), the TCW at tower level was calculated using a scale height of 2.0 km. This approach was also used to estimate pressure at tower level (but with a typical atmospheric scale height about 8.8 km) and for the aerosols with a scale height about 3.0 km. SMARTS spectral transmittance for Rayleigh, Water vapor, Aerosols, Mixed Gas and Trace gas were used for both ground level and tower level to obtain a total transmittance on a vertical path between ground and tower.

Numerical simulations have been done for the whole selected year with an hourly resolution (as MERRA-II input data) to generate transmittance and DNI spectrum for each hour at the two sites. In figures 2 and 3, Total, Rayleigh, water vapor, aerosol, mixed and trace gas transmittance spectrum is represented at noon for the

summer solstice of both sites for two value of α. Main difference of site transmittance is due to the water vapor. Point 1 transitivity of water vapor is close to 0% around 2800 nm even for $\alpha = 1$ (*i.e* tower to ground in vertical path) while it only reach 15% at the same wavelength for Point 2, as shown in Figure 4. Aerosols and Rayleigh transmittance shows some difference between the two sites, affecting wavelength from UV to visible part of spectrum.

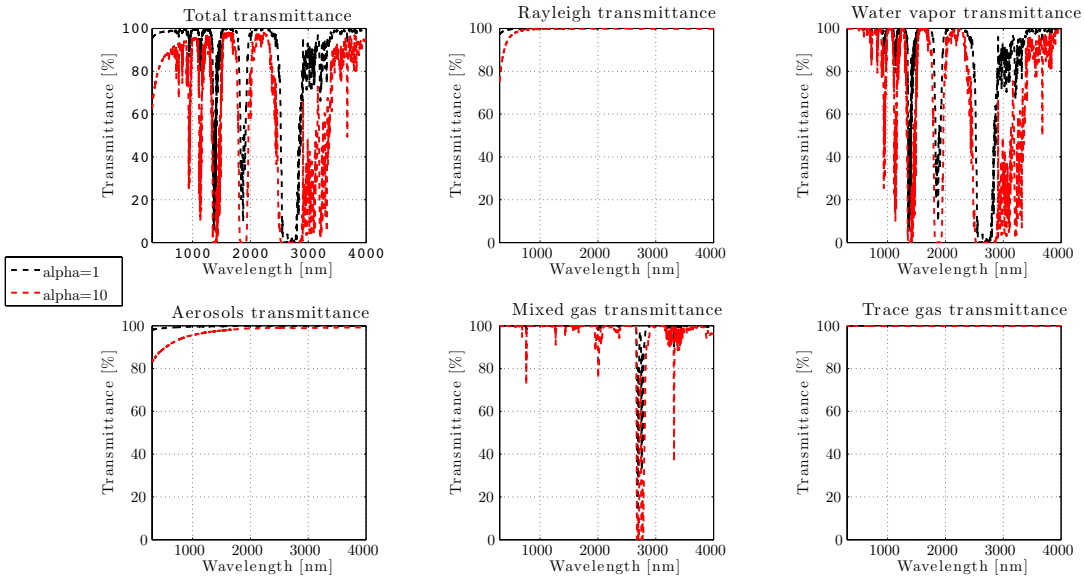

Figure 2 Total, Rayleigh, Water vapor, Aerosols, Mixed gas and Trace gas transmittance at Point 1 (Chilean pacific cost) for summer solstice at noon for two different distances ($\alpha = 1$ and $\alpha = 10$). Spectrums have been calculated with SMARTS and MERRA-II data.

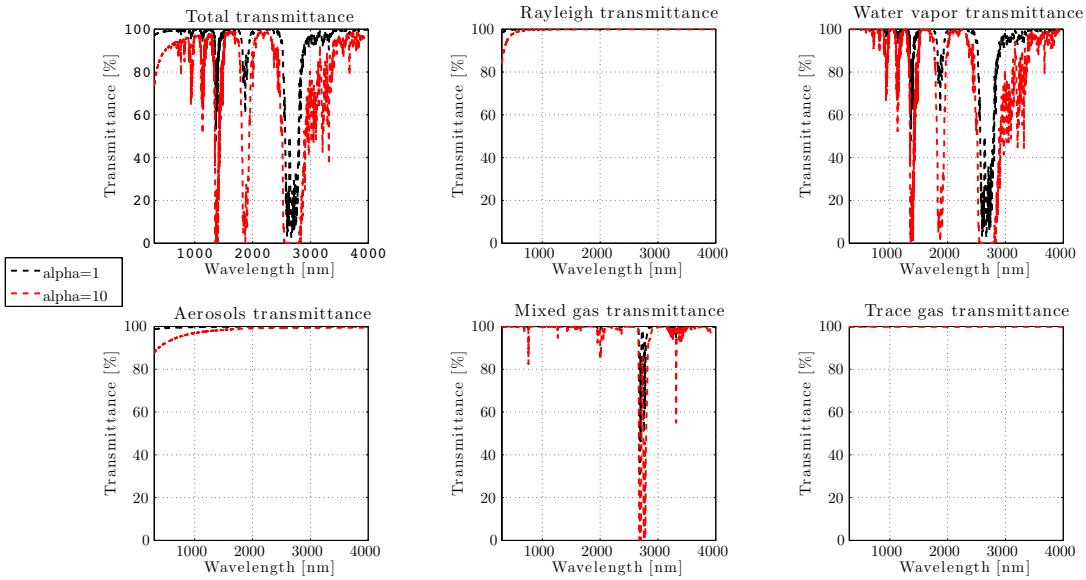

Figure 3 Total, Rayleigh, Water vapor, Aerosols, Mixed gas and Trace gas transmittance at Point 2 (Atacama desert) for the summer solstice at noon for two different distances ($\alpha = 1$ and $\alpha = 10$). Spectrums have been calculated with SMARTS and MERRA-II data.

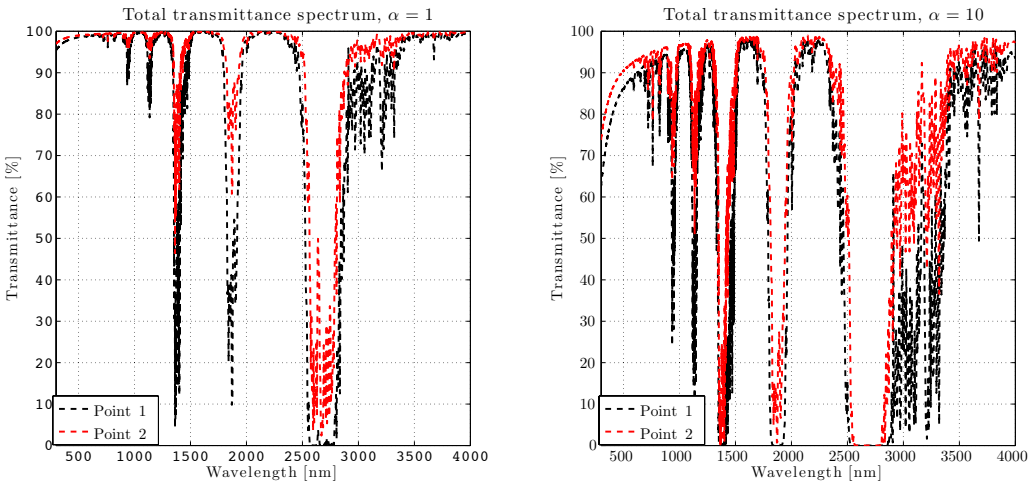

Figure 4 Total transmittance for the two sites at noon of the summer solstice for two different slant distances ($\alpha = 1$ and $\alpha = 10$). Spectrums have been calculated with SMARTS and MERRA-II data.

Spectral attenuation calculated with SMARTS for each hour at the two sites has been integrated around a heliostat field of 8790 heliostats. The heliostat field layer was obtained by using System Advisor Monitoring (SAM) (NREL, 2014) letting us calculate the value of the parameter α for each heliostat. To calculate only the heliostat field attenuation, the Equation 5 is used, whit a constant reflectivity of 100%. Table 2 represents the monthly value of DNI and attenuation at the two sites and Figure 5 shows the monthly variation of atmospheric attenuation at the two sites. The monthly DNI is obtained by summing the hourly DNI while the attenuation is calculated as:

$$\mathcal{A} = \frac{\sum_{t=1}^{t=t_{max}} \left(\sum_{h=1}^{h=8790} \mathcal{A}_\alpha \right) DNI_t}{\sum_{t=1}^{t=t_{max}} DNI_t} \qquad \text{(Eq. 7)}$$

Where t_{max} is the total hour of the month while h represent each heliostat of the heliostat field.

As expected, Point 1 suffers higher atmospheric attenuation than Point 2 (2.5 times higher for the yearly value), mainly due to its location (close to the sea) and elevation. Linked to the atmospheric attenuation, the DNI of Point 1 is 28% lower than Point 2 if we consider the yearly value. Both sites have variations of atmospheric attenuation along the year. At Point 2, from April to October (Winter of South hemisphere) attenuation is low while it is almost two times higher in summer. Point 1 attenuation is more stable even if some high value can be observed in February and October.

Knowing the atmospheric attenuation, it is possible to estimate the impact on the yearly-generated power for this power plant. Here again, SAM has been used to estimate for those two sites the losses on generated power due to atmospheric attenuation and therefore the Levelized Cost Of Electricity (LCOE). Point 1 shows an increase of LCOE about 7.2% while Point 2 increase is 2.6% in comparison to the same cases without any atmospheric attenuation. Even if the variation of LCOE is close to the atmospheric attenuation, there is some difference. This is due that the complete process of generation involved in a tower power plant is not a linear function of the DNI and therefore a decreased of DNI can leads to an higher decrease of produced energy.

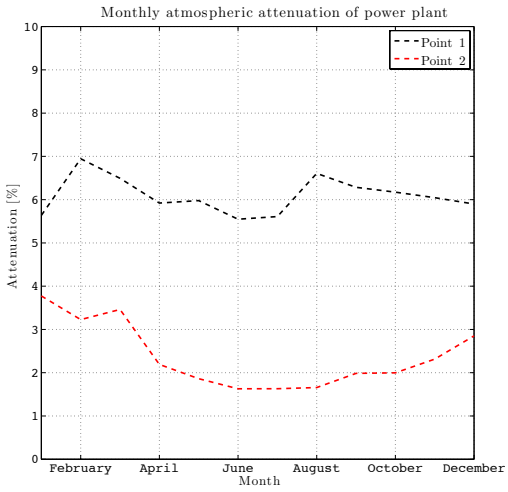

Figure 5 Monthly atmospheric attenuation two sites for the whole heliostat field. Attenuation has been calculated with SMARTS and MERRA-II data considering a 200 m tower and 8700 heliostats.

Tab. 2: Monthly value of DNI and atmospheric attenuation at the two sites. Yearly value is also written at the end of the table.

Month	**Point 1**		**Point 2**	
	DNI $[kWh.m^{-2}]$	Attenuation [%]	DNI $[kWh.m^{-2}]$	Attenuation [%]
January	285.8	5.6	341.8	3.7
February	227.8	6.9	305.9	3.3
March	234.3	6.5	309.8	3.4
April	211.9	5.9	303.3	2.2
May	189.3	6.0	285.1	1.9
June	175.6	5.5	265.2	1.6
July	186.2	5.6	279.6	1.6
August	194.6	6.6	311.0	1.7
September	220.1	6.3	321.3	1.9
October	255.1	6.2	359.1	2.0
November	265.6	6.1	364.5	2.3
December	275.2	5.9	360.7	2.8
Yearly	**2721.9**	**6.1**	**3807.7**	**2.4**

5. Conclusions

Physical description of atmospheric attenuation has been developed from the single tower to ground attenuation. This way to describe attenuation allows simple but physically exact calculation of heliostat field attenuation by taking into account heliostat distance and spectral attenuation. This application of the radiative transfer theory can be applied to estimate local atmospheric attenuation of a Solar Central Receiver power plant. The theory shows that only three parameters are needed to estimated whole heliostat field attenuation: the transmittance spectrum between tower and ground in vertical path, the heliostat-receiver distance and DNI spectrum at ground level. By combining those three parameters, theory shows that the atmospheric attenuation can be calculated exactly for the whole heliostat field. This theory can be applied to any kind of atmosphere at the condition that

atmosphere extinction coefficient is homogenous in the horizontal plane but not necessary in the vertical direction. It has been shown that derived transmittance spectrum should be considered with the actual DNI spectrum, to keep the mathematical calculation exact.

An application of the theory has been made by using numerical methods to estimate transmittance spectrum, heliostat attenuation and DNI spectrum. Any atmospheric radiative model that allows spectral calculation (such as ModTran (Berk et al., 2006), LibRadTran (Emde et al., 2016) or SMARTS) could be used to estimate whole heliostat field attenuation. As an example, an application has been made using SMARTS model and MERRA-II database to study heliostat field attenuation for two sites in Chile and a 200 meters tower power plant. In this study, such power plant located near the pacific cost would suffer about 6% of atmospheric attenuation while if it is located in the Atacama Desert, this attenuation would be only 2.4%. Knowing the atmospheric attenuation of a tower power plant can help to design efficient heliostat field and have best estimation of its Levelized Cost Of Energy. At the two sites, using System Advisor Monitor, it has been shown that variation in atmospheric attenuation is a good indicator of LCOE variation, but a full calculation taking into account whole power plant process need to be done to estimate accurately this variation.

6. Acknowledgments

The authors acknowledge the generous financial support provided by the Chilean Economic Development Agency (CORFO) under the project 13CEI2-21803 and the Innova Chile – CORFO project 17BPE3-83761. Mercedes Ibarra also acknowledges CONICYT/FONDAP/15110019 “Solar Energy Research Center” SERC-Chile.

The authors would like to thanks Christian Gueymard for letting available as free software the radiative model (SMARTS) used in this work. We also thank the NASA for the recollection and maintenance of the MERRA-II database.

7. References

Ballestrín, J., Marzo, A., 2012. Solar radiation attenuation in solar tower plants. Sol. Energy. https://doi.org/10.1016/j.solener.2011.10.010

Berk, A., Anderson, G.P., Acharya, P.K., Bernstein, L.S., Muratov, L., Lee, J., Fox, M., Adler-Golden, S.M., Chetwynd, Jr., J.H., Hoke, M.L., Lockwood, R.B., Gardner, J.A., Cooley, T.W., Borel, C.C., Lewis, P.E., Shettle, E.P., 2006. MODTRAN5: 2006 update. https://doi.org/10.1117/12.665077

Bosilovich, M., Akella, S., Coy, L., Cullather, R., Draper, C., Gelaro, R., Kovach, R., Liu, Q., Molod, A., Norris, P., Wargan, K., Chao, W., Reichle, R., Takacs, L., Vikhliaev, Y., Bloom, S., Collow, A., Firth, S., Labow, G., Partyka, G., Pawson, S., Reale, O., Schubert, S.D., Suarez, M., 2015. MERRA-2 : Initial Evaluation of the Climate. NASA Tech. Rep. Ser. Glob. Model. Data Assim. https://doi.org/NASA/TM–2015-104606/Vol. 43

Ebrahimpour, A., Maerefat, M., 2010. A method for generation of typical meteorological year. Energy Convers. Manag. https://doi.org/10.1016/j.enconman.2009.10.002

Emde, C., Buras-Schnell, R., Kylling, A., Mayer, B., Gasteiger, J., Hamann, U., Kylling, J., Richter, B., Pause, C., Dowling, T., Bugliaro, L., 2016. The libRadtran software package for radiative transfer calculations (version 2.0.1). Geosci. Model Dev. https://doi.org/10.5194/gmd-9-1647-2016

Gueymard, C.A., 2001. Parameterized transmittance model for direct beam and circumsolar spectral irradiance. Sol. Energy. https://doi.org/10.1016/S0038-092X(01)00054-8

Gueymard, C.A., López, G., Rapp-Arrarás, I., 2017. Atmospheric transmission loss in mirror-to-tower slant ranges due to water vapor, in: AIP Conference Proceedings. https://doi.org/10.1063/1.4984518

NREL, 2014. System advisor model, sam 2014.1. 14: General description, National Renewable Energy Laboratory,NREL.